Supplemental Document

Biomedical Optics EXPRESS

Quasi-analytic solution for real-time multi-exposure speckle imaging of tissue perfusion: supplement

DANIEL A. RIVERA AND CHRIS B. SCHAFFER

Nance E. and Peter C. Meinig School of Biomedical Engineering, Cornell University, Ithaca, NY, USA

Supplement DOI: https://doi.org/10.6084/m9.figshare.23581881

Parent Article DOI: https://doi.org/10.1364/BOE.493821

A QUASI-ANALYTIC SOLUTION FOR REAL-TIME MULTI-EXPOSURE SPECKLE IMAGING OF TISSUE PERFUSION: SUPPLEMENTAL DOCUMENT

Methods

Animal preparation

All animal procedures were approved by the Cornell Institutional Animal Care and Use Committee (protocol 2015-0029) and were performed under the guidance of the Cornell Center for Animal Resources and Education. Adult C57BL/6 mice (n = 2) at 3 and 9 months of age were used.

Mice were induced under anesthesia using 3% isoflurane in 100% oxygen, moved to a stereotactic frame, and maintained at 1-2% isoflurane during surgical procedures. Body temperature was regulated with a feedback-controlled DC temperature controller and heating pad (40-90-8D, FHC). Puralube vet ointment was applied to each eye and reapplied as necessary. Mice received ketoprofen (5 mg/kg, 2.0 mg/mL) and dexamethasone (0.2 mg/kg, 0.1 mg/mL) to reduce inflammation from the removal of the skull and glycopyrrolate (0.2 mg/mL, 20 mg/kg, West-Ward Pharmaceuticals) to reduce respiratory secretions. The fur on the scalp was shaved and the area cleaned with alternating iodine and 70% ethanol solutions. Prior to any incisions, 100 μL of bupivacaine (0.1% solution) was administered into the incision site as a local anesthetic. The mice received ~5-mm diameter craniotomies between lambda and bregma using a 0.7-mm dental drill, followed by placement of an 8-mm diameter cover glass. Sterile saline was added to the surface of the brain before securing the cover glass to the dried skull surrounding the craniotomy with cyanoacrylate (Loctite). Dental cement sealed the craniotomy to restore intracranial pressure and maintain sterility. One mouse was allowed 3 weeks for recovery before imaging. A photothrombotic stroke was induced acutely in the second mouse.

Multi-exposure speckle imaging

For imaging, the mice were induced under 3% isoflurane in 20% oxygen, placed in a stereotactic frame, and maintained at 1-2% isoflurane while monitoring respiratory and heart rate via the piezoelectric sensor. Body temperature was regulated with a feedback-controlled heating pad. Puralube vet ointment was applied to each eye and reapplied as necessary. Mice were injected subcutaneously with glycopyrrolate. For the first mouse, 30 images for each of the standard exposure times were taken at 12-bit resolution in a cyclical manner. The raw images were processed into speckle contrast images using a 7×7 window, then averaged into a single 2000×2000×15 speckle contrast matrix. An additional 10 speckle images were averaged for each of the 20 extended exposure times between 20 μs and 650 ms with the same resolution and bit-depth to produce a 2000×2000×20 speckle contrast matrix. For the induced photothrombotic stroke, the photothrombotic set of exposures were taken at ~1.5-2 Hz for at least 5 minutes. Exposure times are listed in Table S1. Imaging was performed in MATLAB 2019b on an Intel® Core™ i7-7700T CPU @ 2.90 GHz system running Windows 10. Processing was done in MATLAB 2021a on an Intel® Xeon® CPU E5-2687W v4 @ 3.00GHz 24-core system running Ubuntu OS.

Table S1. Exposure times used in each experiment and simulation

Experimental Protocol	Exposures (ms)
Standard exposures	0.05, 0.075, 0.10, 0.25, 0.50, 0.75, 1.0, 2.5, 5.0, 7.5, 10, 25, 40, 50, 80
Simulated log-spaced exposures	0.05, 0.085, 0.14, 0.24, 0.41, 0.70, 1.2, 2.0, 3.4, 5.7, 9.7, 16, 28, 47, 80
Extended exposures	0.02, 0.035, 0.06, 0.10, 0.18, 0.31, 0.53, 0.92, 1.6, 2.7, 4.7, 8.2, 14, 24, 42, 73, 130, 220, 380, 650
Photothrombosis exposures	0.02, 0.036, 0.065, 0.12, 0.21, 0.39, 0.70, 1.3, 2.3, 4.1, 7.5, 14, 24, 44, 80

Induction of a photothrombotic stroke

For induction of a photothrombotic stroke, we used a Rose Bengal solution (10 mg/mL) which photochemically produces reactive oxygen species in the presence of light, with a continuous-wave green laser (λ = 532 nm) (Compass 215M-50, Coherent) as the illumination source. A series of neutral density filters reduced the power to ~1-2 mW at the imaging plane and a 520/40 nm optical filter (ThorLabs) removed residual NIR light from the green laser so as not to interfere with the speckle imaging. A 200-mm focal length lens focused the beam down to ~500-μm diameter while a periscope steered the beam to a target location (Fig. 5A). The green beam was placed over an arteriole using a laser speckle contrast map of the vasculature as reference (Fig. 5B-C, green *X*). Once positioned, the beam was blocked before retro-orbitally injecting the mouse with 50 μL of Rose-Bengal solution. Image acquisition began 30-60 s prior to unblocking the green diode laser to induce clotting. The green laser remained unblocked for 60 s with the times of illumination onset and termination marked on the DAQ board by a short TTL pulse.

Nonuniform moving average filter

For unequally-spaced data in the logarithmic domain typically used in the literature, a nonuniform moving average filter with a total width of 1 decade, or 0.5 decades across the center point, was applied to reduce system measurement noise. The points within range are weighted by the distance to the center timepoint as $wt = (\frac{w}{2} - |T - T_{center}|)$ and the filter applied as

$$K_f^2(T_{center}) = \frac{\sum_i^I K_i^2 wt_i}{\sum_i^I wt_i} \tag{S1}$$

Polynomial expansions

Table S2 shows the coefficients for the 10th order polynomial expansion of the speckle contrast derivative relative to ρ, which is used to reduce computational overhead in determining the scattering model in Step 4 from Fig. 2.

Table S2. Polynomial expansion of $dK^2(T_{peak})/d\ln(T)$ as a function of ρ

Multiple-Ordered		Multiple-Unordered	
x^n	c_n	x^n	c_n
10	-0.020475343735539	10	0.053297852491085
9	-0.000249703516762	9	-0.267813703593650
8	0.193138590579442	8	0.529732554893485
7	-0.360479187939359	7	-0.522690178203463
6	0.282977235939114	6	0.299320834277943
5	-0.159691928427907	5	-0.130682424041211
4	0.008759628227216	4	-0.002907089625296
3	-0.042800145778791	3	-0.039727987048522
2	0.740574034436267	2	0.463936419535563
1	-1.283491167540141	1	-0.764925668142888
0	0.000000130185034	0	0.000000051719825

Derivatives of the speckle decorrelation function with respect to ln(T)

Our function, y, is the function for speckle contrast.

$$y = K^2(\tau_c,\beta,\rho,D_{MU}) \tag{S2}$$

We intend to take the derivative with respect to ln(T). To do so, we set a function, u, as:

$$u = \ln(T) \tag{S3}$$

in order to take the derivative such that

$$\frac{dy}{d\ln(T)} = \frac{dy}{du} \tag{S4}$$

Applying a chain rule, we find

$$\frac{dy}{du} = \frac{dy}{dT}\frac{dT}{du} \tag{S5}$$

We rearrange Eq. S3 so that

$$T = e^u \rightarrow \frac{dT}{du} = e^u \tag{S6}$$

Combining Eq. S5 and Eq. S6, we get

$$\frac{dy}{du} = \left(\frac{dy}{dT}\right)(e^u) = \left(\frac{dy}{dT}\right)(T) \tag{S7}$$

The term, e^u, can be substituted with T based on Eq. S6. We can now apply Eq. S7 to obtain the derivatives of the decorrelation function with respect to ln(T). For Eq. 10, the derivative with respect to T gives

$$\frac{d}{dT}K_{ves}^2 = \beta\begin{pmatrix} \rho^2\left(e^{-2x}\left(-\frac{\tau_c^2}{T^3}-\frac{\tau_c}{T^2}\right)+\frac{\tau_c^2}{T^3}-\frac{\tau_c}{T^2}\right)+ \\ 4\rho(1-\rho)\left(e^{-x}\left(-\frac{2\tau_c^2}{T^3}-\frac{\tau_c}{T^2}\right)+\frac{2\tau_c^2}{T^3}-\frac{\tau_c}{T^2}\right)\end{pmatrix} \tag{S8}$$

As seen in Eq. S8, the relation between τ_c and T is no longer linear as the exponents of T are larger than those of τ_c. However, multiplying by T, as in Eq. S7, reduces the exponents of T to match those of τ_c, restoring the relation of $x = T/\tau_c$ from Eq. 10 and Eq. 12.

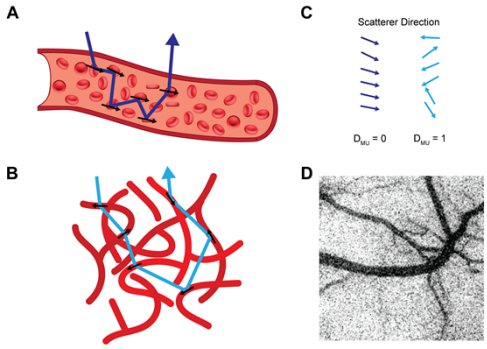

Fig. S1. Schematic of the multiple scattering models for vascular and parenchymal regions. (A) Model vessel representing multiple scattering of a photon on scatterers moving in an ordered direction. (B) Example of a capillary bed with photons scattering off cells moving in random directions. (C) Arrows representing the scatterers' direction of movement and indicating the appropriate scattering model to capture the dynamics. Colors correspond to the photon path color in A and B. (D) Scattering model coefficient of a processed multi-exposure image using sREMI. Vessels are near zero (black), with a gradient moving outward from the vessels to parenchyma, where the coefficient approaches one (white).

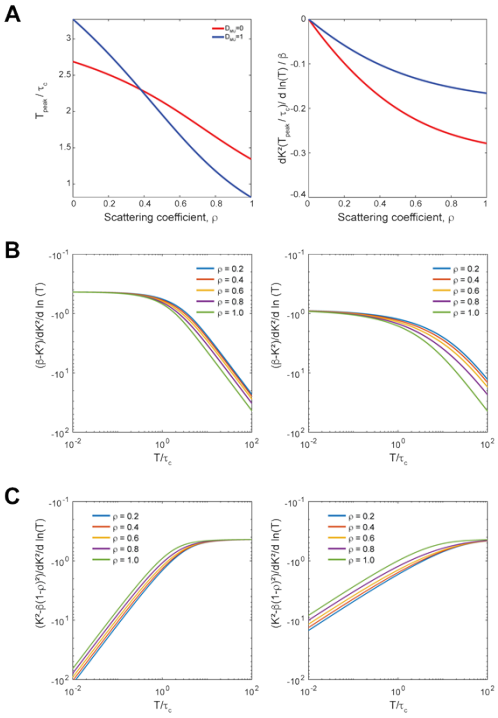

Fig. S2. Influence of dynamic scattering on function behavior. (A) Lateral translation in differential peak location (left) and peak amplitude (right) as a function of ρ for multiple-ordered scattering (red) and multiple-unordered scattering models (blue). (B) Lateral translation in ratio of $(K^2(0)-K^2(T))$ to $dK^2(T)/d\ \ln(T)$ with respect to τ_c for various ρ for multiple-ordered scattering (left) and multiple-unordered scattering (right). (C) Lateral translation in ratio of $(K^2(T)-K^2(\infty))$ to $dK^2(T)/d\ \ln(T)$ with respect to τ_c for various ρ for multiple-ordered scattering (left) and multiple-unordered scattering (right).

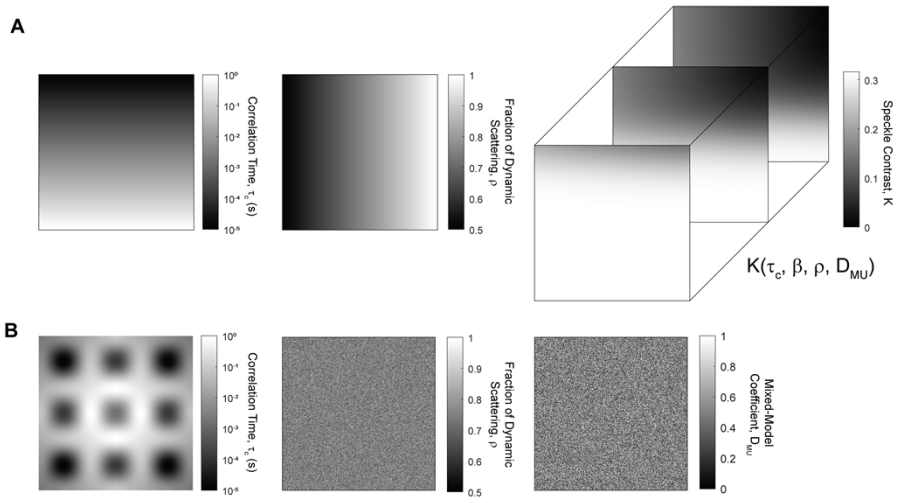

Fig. S3. Spatial maps for simulated testing data. (A) Maps for correlation times (τ_c, left) and fraction of dynamic scattering coefficients (ρ, middle) used to produce full-spectrum speckle contrast matrices (right). β is set as 0.10 and D_{MU} is set to 0 for this example. (B) Spatially varying correlation time map (τ_c, left), randomized fraction of dynamic scattering coefficients (ρ, middle) and randomized scattering model coefficient (D_{MU}, right) for testing sREMI.

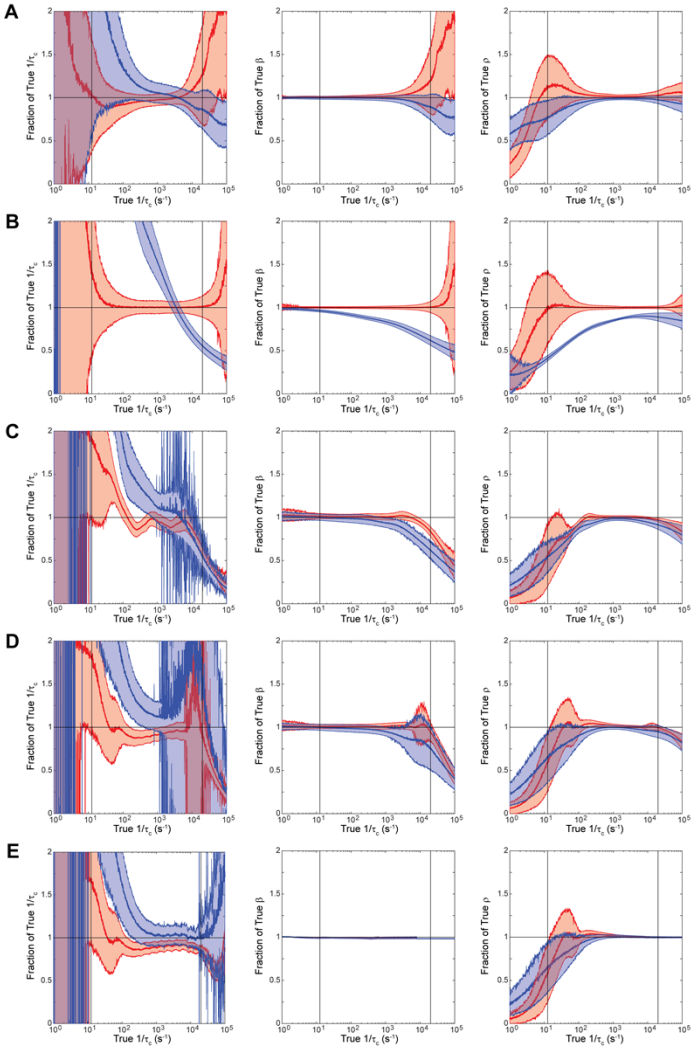

Fig. S4. Performance of processing methods on simulated data with artificial noise. Plots of estimated correlation times, τ_c (left), the normalization coefficient, β (middle), and the fraction of dynamic scattering, ρ (right), all normalized to the true value, vs. true correlation times for (A) mm-MESI, (B) sm-MESI, (C) REMI using typical exposure times, (D) REMI using logarithmically spaced exposure times, and (E) sREMI using logarithmically spaced exposure times. Red traces correspond to multiple-ordered scattering data; blue traces correspond to multiple-unordered scattering data. Shaded regions represent standard deviations from log-space values. Vertical dashed lines represent the bounds set by the exposure times.

Supplementary Movie 1. sREMI output during mild photothrombotic stroke at 1-mW exposure. Green square indicates the illumination of the target arteriole by the green diode laser.

Supplementary Movie 2. sREMI output during moderate photothrombotic stroke at 2-mW exposure. Green square indicates the illumination of the target arteriole by the green diode laser.